Article

Chinese Science Bulletin

SPECIAL TOPIC: Nanobiotechnology

November 2013 Vol.58 No.33: 4051–4056
doi: 10.1007/s11434-013-6023-8

Preparation and upconversion luminescence cell imaging of *O*-carboxymethyl chitosan-functionalized $NaYF_4$:Yb^{3+}/Tm^{3+}/Er^{3+} nanoparticles

LI Hao & WANG LeYu*

Key Laboratory of Chemical Resource Engineering, College of Science, Beijing University of Chemical Technology, Beijing 100029, China

Received April 1, 2013; accepted May 22, 2013; published online August 8, 2013

Upconversion luminescence nanoparticles (UCNPs) have shown promising applications in biomedical fields as luminescent probes because of their excellent advantages such as single excitation with multicolor emission, low autofluorescence, and deep penetration. But the biological applications of such nanomaterials are still restricted due to the unfavorable surface properties. In this work, we develop a facile one-pot hydrothermal route to obtain *O*-carboxymethyl chitosan (OCMC)-wrapped $NaYF_4$:Yb^{3+}/Tm^{3+}/Er^{3+} red UCNPs which have been used for targeted cell luminescence imaging directly and efficiently. The successful coating of the UCNPs by OCMC has been confirmed by Fourier-transform infrared (FTIR) spectroscopy and dynamic light scattering (DLS) studies. Transmission electron microscopy (TEM), powder X-ray diffraction (XRD), thermogravimetric analysis (TGA), and photoluminescence (PL) spectra have been used to characterize the size, composition and emission color of the samples, respectively. Due to the good biocompatibility, water-solubility, and strong UC luminescence, these hydrophilic nanocrystals will open up new avenues in further bioapplications.

water-stable, $NaYF_4$ nanoparticles, upconversion luminescence, cell-imaging

Citation: Li H, Wang L Y. Preparation and upconversion luminescence cell imaging of *O*-carboxymethyl chitosan-functionalized $NaYF_4$:Yb^{3+}/Tm^{3+}/Er^{3+} nanoparticles. Chin Sci Bull, 2013, 58: 4051–4056, doi: 10.1007/s11434-013-6023-8

Upconversion (UC) luminescence nanomaterials are a new class of luminescent probes under intense research and development for broad applications *in vitro* [1–3], and *in vivo* imaging [4–8] because of their advantages such as minimal background autofluorescence and photobleaching (NIR excitation) [9,10], high room-temperature quantum yields [11], and long luminescence life times [12]. As we know, sodium yttrium fluoride ($NaYF_4$) is the most efficient UC host materials for UC luminescence [13,14]. As bio-probes for imaging and detection, conceivable advantages include low toxicity [15], good photostability [16,17], sharp absorption and emission lines [18], and multicolor emission [19–21] had been reported. Recent research has achieved considerable success in synthesizing UCNPs for bio-imaging [22–24]. However, the surface modification via silica coating [25–28], ligand exchange [29,30], and ligand oxidation [31,32] to render the hydrophobic nanoparticles water dispersible may lead to time-consuming and weak luminescence. Therefore, it is very important to develop a facile one-pot strategy for the synthesis of UCNPs with strong UC luminescence, good water stability, and excellent biocompatibility.

To the best of our knowledge, chitosan is one of the most naturally occurring biopolymers and has many meaningful biological properties such as biocompatibility, biodegradability, low toxicity, good availability, and antibacterial activities toward mammalian cells. Some chitosan derivatives such as *O*-carboxymethyl chitosan (OCMC) exhibit even more excellent biological activity [33] and water stability. Herein, the OCMC was used as coating agent to fabricate $NaYF_4$:Yb^{3+}/Tm^{3+}/Er^{3+} nanocrystals via a simple and mild hydrothermal process. As shown in Scheme 1, the effectiveness of such OCMC-functionalized nanocrystals for UC luminescence bioimaging has been evaluated on HeLa

*Corresponding author (email: lywang@mail.buct.edu.cn)

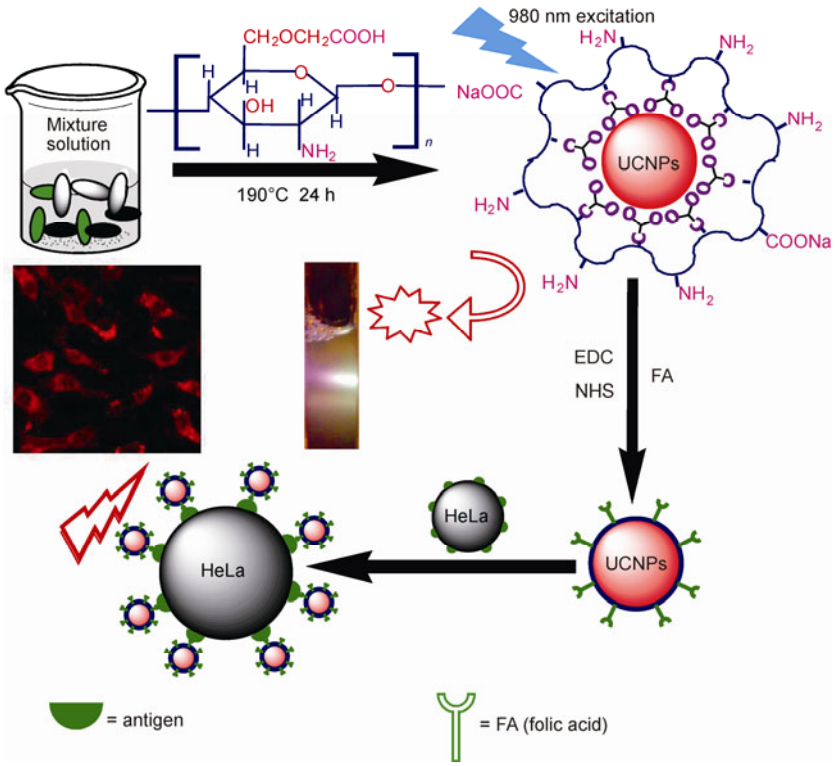

Scheme 1 Schematic diagram for the synthesis and red UC luminescence cell imaging of OCMC coated $NaYF_4$:Yb^{3+}/Tm^{3+}/Er^{3+} nanoparticles.

cancer cell successfully.

1 Experimental

1.1 Materials

$Y(NO_3)_3 \cdot 6H_2O$, $Er(NO_3)_3 \cdot 6H_2O$, $Yb(NO_3)_3 \cdot 6H_2O$, and $Tm(NO_3)_3 \cdot 6H_2O$ were obtained from Beijing Ouhe Chemical Reagent Company. NaF, NaOH, ethanol, ethylene glycol, and paraformaldehyde were purchased from Beijing Chemical Reagents Company. Dimethyl sulfoxide (DMSO) and 1-ethyl-3-(3-dimethly-aminopropyl) carbodiimide (EDC) were obtained from Aldrich. EDC and *N*-hydroxysuccinimide (NHS, Acros) were used for bioconjugation. Methyl thiazolyl tetrazolium (MTT) was obtained from Amresco and used for the cytotoxicity assay of the nanomaterials. Folic acid (FA) and OCMC were purchased from Beijing Aoboxing biotech. All the chemicals were of analytical grade and used as received without further purification. Deionized water was used throughout.

1.2 Particle characterization

The morphology and size of the as-prepared nanoparticles were checked on a JEOL JEM-1200EX transmission electron microscope (TEM) with a tungsten filament at an accelerating voltage of 100 kV. Dynamic light scattering (DLS) particle size analysis was recorded with a Malvern Mastersize 2000 zeta and size analyzer. X-ray diffraction (XRD) patterns were examined on a Rigaku XRD-A112 X-ray diffractometer which employed Cu Kα radiation of wavelength λ = 1.5418 Å. The operating current and voltage were kept at 40 mA and 40 kV, respectively. A 2θ range from 10° to 80° was covered in steps of 0.02° with a count time of 2 s. The emission spectra of the UCNPs were measured via a Hitachi F-4600 fluorescence spectrophotometer equipped with a 980-nm diode laser for irradiation. Fourier-transform infrared (FTIR) spectra were performed on a JASCO FT/IR-460 PLUS spectrometer (Tokyo) at room temperature. The thermogravimetric analysis (TGA) was carried out on a Simultaneous thermal analyzer TGA/DSC 1/1100 SF (METTLER TOLEDO). The cell imaging was performed on a TCS SP5 two-photon Confocal Microscopy (Leica) equipped with an IR diode laser (MaiTai).

1.3 Synthesis of UCNPs@OCMC

The OCMC-capped $NaYF_4$:Yb^{3+}/Tm^{3+}/Er^{3+} (UCNPs@OCMC) red UC luminescence nanoparticles were synthesized via a one-pot hydrothermal method. In brief, OCMC (0.15 g), NaOH (30 mg), and deionized water (10 mL) were added into an autoclave. After the mixture was stirred at room temperature for 30 min, ethanol (15 mL) and ethylene glycol (10 mL) were added successively. Then, the aqueous solution of $Y(NO_3)_3 \cdot 6H_2O$ (1.59 mL, 0.5 mol/L), $Yb(NO_3)_3 \cdot 6H_2O$ (0.4 mL, 0.5 mol/L), $Tm(NO_3)_3 \cdot 6H_2O$ (0.02 mL, 0.05 mol/L), and $Er(NO_3)_3 \cdot 6H_2O$ (0.08 mL, 0.05 mol/L) were added and the stirring was kept for another 30 min.

The sodium fluoride solution (6 mL, 1.0 mol/L) was then added under stirring. The autoclave was treated at 190°C for 24 h. After the autoclave was allowed to cool to room temperature naturally, the final products were collected and washed with deionized water. This purification cycle was repeated for twice. The final products were dispersed in 4.0 mL deionized water and stored for later use. For the characterization of XRD, FTIR, and TGA, the white powder was dried at 70°C for 10 h.

1.4 Cytotoxicity assay

Cytotoxicity assessment was measured on the HeLa cell line as described earlier with slight modifications [34]. Briefly, the cells were seeded in a 96-well cell culture plate (5×10^4 cells/well) and cultured under recommended conditions at 37°C in a 5% CO_2-humidified incubator overnight to make sure the cells were adherent. The as-prepared UCNPs@OCMC colloidal solution with concentration ranging from 0 to 200 μg/mL was added into each well, respectively. Then, the plate was incubated at 37°C for 24 or 48 h. Finally, the cytotoxicity of the as-prepared nanoparticles was evaluated via MTT assay [24].

1.5 Cell imaging

The UC luminescence imaging was conducted on a TCS SP5 two-photon Confocal Microscopy (Leica) equipped with a MaiTai IR laser. HeLa cancer cells were seeded on a sterilized glass cover slide and cultured in a 6-well cell culture plate overnight under recommended conditions at 37°C in 5% CO_2-humidified incubator. The as-prepared FA bioconjugated UCNPs (UCNPs@OCMC-FA) stock solution was added into the cell culture well with a concentration of 75 μg/mL. Then the cells were cultured for another 4 h before the removal of unattached UCNPs by washing with buffer. As a control, the UCNPs@OCMC without FA modification was incubated with the HeLa cells under the same conditions. Then the cells on the glass slide were washed with PBS and fixed in 4% paraformaldehyde solution for 15 min.

2 Results and discussion

2.1 TEM and DLS analysis of UCNPs@OCMC

TEM was used to evaluate the morphology and particle size distribution (PSD) of the OCMC-capped $NaYF_4$:Yb^{3+}/Tm^{3+}/Er^{3+} nanoparticles. As shown in TEM images (Figure 1(a) and (b)), the obtained nanoparticles are spherical in shape and relatively monodisperse. The particle size determined by random measurements of 200 particles is 317.15 ± 6.06 nm (Figure 1(c)). The DLS experiments were also conducted on the same colloidal solution to ascertain the PSD (Figure 1(d)). The results showed that these UCNPs have a narrow PSD with a hydrodynamic size of 335.15 ± 4.18 nm,

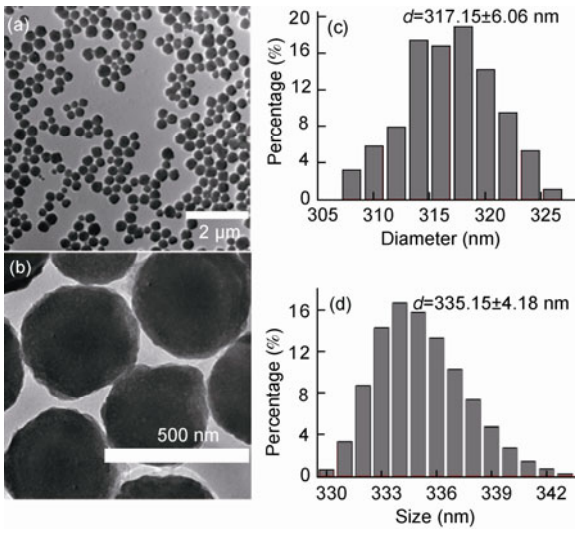

Figure 1 TEM images ((a) and (b)) and size distribution ((c) and (d)) of the UCNPs@OCMC. (c) Particle size distribution calculated from the TEM image, (d) DLS size distribution of OCMC-coated $NaYF_4$:Yb^{3+}/Tm^{3+}/Er^{3+} UCNPs dispersed in water.

which is in correspondence with the calculated size. It is notable that, due to OCMC coating and the particle-solvent interaction [35], the DLS particle size is slightly larger than the TEM particle size.

2.2 Powder XRD analysis

The as-synthesized nanocrystals have been characterized by XRD technology. As shown in Figure 2, it is evident that the main peak positions and relative intensities agree well with the data reported in standard face-centered cubic phase $NaYF_4$ (JCPDS card No. 77-2042). Meanwhile, other weak diffraction peaks are in accordance with the standard patterns of hexagonal phase $NaYF_4$ (JCPDS card 16-0334). The results indicated that the UCNPs consist of cubic phase (major) and hexagonal phase (minor) $NaYF_4$. In addition,

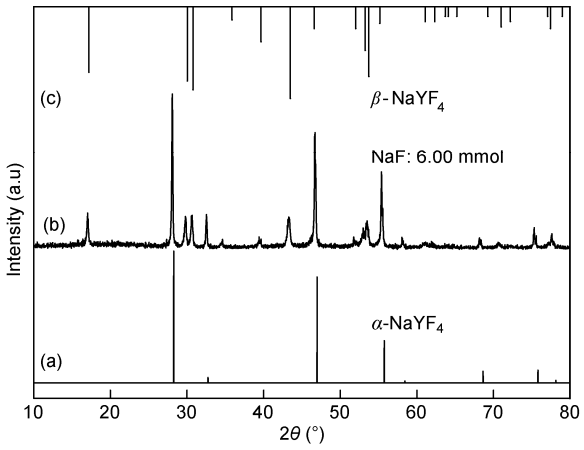

Figure 2 Powder XRD patterns of (a) standard cubic phase $NaYF_4$ (JCPDS card 77-2042), (b) the as-synthesized nanoparticles, and (c) standard hexagonal phase $NaYF_4$ (JCPDS card 16-0334).

from the sharp and high diffraction peaks in the XRD patterns, we can deduce that the samples are well crystallized.

2.3 Upconversion luminescence spectra

The OCMC coated $NaYF_4$:Yb^{3+}/Tm^{3+}/Er^{3+} nanocrystals emit bright-red luminescence under 980 nm excitation. As depicted in Figure 3(a), the emission peaks of the as-prepared nanoparticles in the wavelength region of 300–900 nm are assigned to the transitions of $^1G_4 \rightarrow {}^3H_6$ (Tm^{3+}: 478 nm), $^3H_4 \rightarrow {}^3H_6$ (Tm^{3+}: 808 nm), $^2H_{11/2} \rightarrow {}^4I_{15/2}$ (Er^{3+}: 529 nm), $^4S_{3/2} \rightarrow {}^4I_{15/2}$ (Er^{3+}: 545 nm), and $^4F_{9/2} \rightarrow {}^4I_{15/2}$ (Er^{3+}: 658 nm), respectively [21,36]. The inset of Figure 3(a) showed the corresponding red UC luminescence photographs of UCNPs dispersed in water. In order to determine the number of photons in the UC process of the as-prepared nanocrystals, the intensities of the UC emissions were recorded as a function of the 980 nm excitation intensity. The slope of the plot in Figure 3(b) is about 2, indicating a two-photo excitation progress.

2.4 FTIR spectra and TGA analysis of $NaYF_4$:Yb^{3+}/Tm^{3+}/Er^{3+} nanoparticles

FTIR spectra of UCNPs, OCMC, and UCNPs@OCMC were showed in Figure 4. $NaYF_4$:Yb^{3+}/Tm^{3+}/Er^{3+} UCNPs prepared in the absence of OCMC shows no characteristic adsorption peaks of pure OCMC (Figure 4(a)). Three strong peaks at 1605, 1420, and 1083 cm^{-1} (Figure 4(b)), corresponding to the N–H bending vibration, COO^- symmetrical stretching vibrations, and C–O bending vibration, respectively, were found in the FTIR spectrum of OCMC [37]. The FTIR spectrum of UCNPs@OCMC (Figure 4(c)) is highly consistent with that of OCMC strongly suggesting that the OCMC has been successfully coated onto the UCNPs. The surface coating of UCNPs@OCMC was further investigated by TGA with heating rate of 10°C/min in the range of 35–800°C under N_2 atmosphere. Figure 5 illustrated the TGA weight for as- prepared UCNPs@OCMC and the weight loss is 11%. The first slow weight loss at 40–150°C can be explained by the evaporation of absorbed water molecules. The sharp weight loss at 270–600°C can be attributed to the thermal decomposition of the coating OCMC on the UCNPs. The results further inferred that OCMC has been coated onto the surface of UCNPs, which is in accordance with the FTIR results shown in Figure 4.

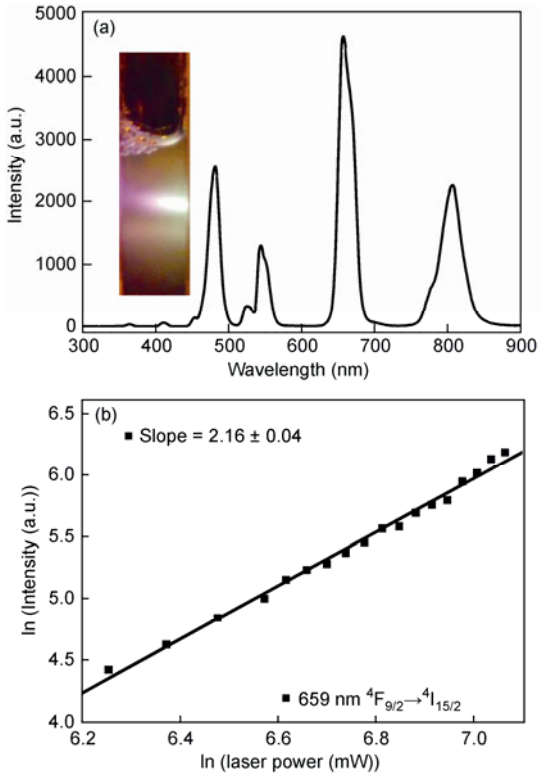

Figure 3 (a) UC luminescence emission spectra of $NaYF_4$:Yb^{3+}/Tm^{3+}/Er^{3+} nanoparticles. Inset: digital photos of the UCNPs dispersed in water with the irradiation power at 1.2 W (980 nm). (b) Power dependence of UCNPs emission intensities of $^4F_{9/2} \rightarrow {}^4I_{15/2}$ transition in $NaYF_4$:Yb^{3+}/Tm^{3+}/Er^{3+} sample under 980 nm laser excitation.

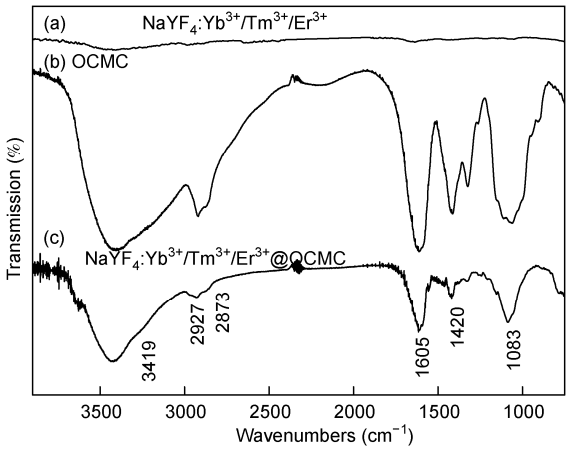

Figure 4 FTIR spectra of $NaYF_4$:Yb^{3+}/Tm^{3+}/Er^{3+} nanoparticles (a), OCMC (b), and UCNPs@OCMC nanoparticles (c).

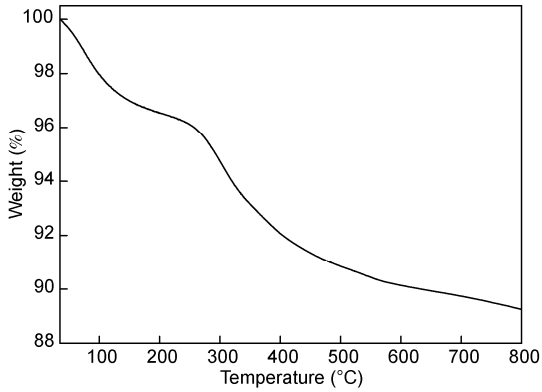

Figure 5 TGA curve of $NaYF_4$:Yb^{3+}/Tm^{3+}/Er^{3+}@OCMC nanoparticles.

2.5 Cytotoxicity and cell imaging

To demonstrate their potential bioapplications, the cytotoxicity of UCNPs@OCMC was carried out using MTT assay on HeLa cell lines. As shown in Figure 6, no significant difference in cell viability was observed when the concentrations of UCNPs@OCMC ranged from 0 to 75 μg/mL after incubation for 24 h. Even though the concentration went up to as high as 200 μg/mL, cell viabilities were still greater than 85%. Even after incubation with NPs (200 μg/mL) for 48 h, the cell viability was still over 78%. These results fully showed that UCNPs@ OCMC demonstrates good biocompatibility, which is highly desirable for subsequent cell imaging application.

As a proof of concept, OCMC coated UCNPs were used for UC luminescence imaging on HeLa cell. As shown in Scheme 1, by means of EDC and NHS, OCMC-functionalized UCNPs were bioconjugated with FA, which involved a condensation reaction between carboxyl groups of FA and amino groups of OCMC. Then the FA bioconjugated UCNPs were utilized for the UC luminescence cell imaging. As depicted in Figure 7(a1)–(a3), the HeLa cells exhibited bright-red UC luminescence according to the attachment of UCNPs@OCMC-FA through the specific interaction between the FA and the antigen protein on the HeLa cell surface. As a control, the UCNPs@OCMC without FA bioconjugation could not stain the HeLa cells and no red luminescence could be observed on the HeLa cell surface (Figure 7(b1)–(b3)), indicating the non- specific adsorption of UCNPs was negligible. The results clearly demonstrate that the as-prepared water-dispersible and biocompatible UCNPs will be promising candidates for targeted bioimaging and other bioapplications.

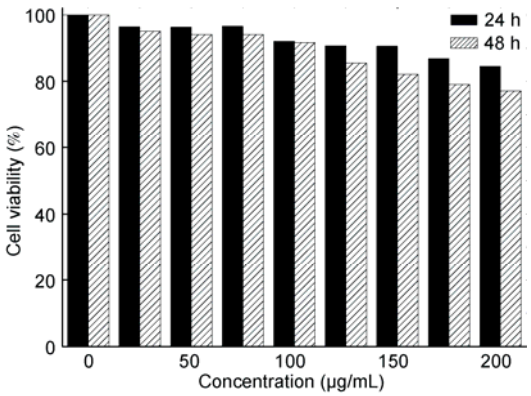

Figure 6 Cell viability test of HeLa cell lines incubated with different concentration of $NaYF_4:Yb^{3+}/Tm^{3+}/Er^{3+}$@OCMC UCNPs at 37°C for 24 and 48 h, respectively.

3 Conclusion

A facile one-pot strategy has been successfully developed for the preparation of water-dispersible, biocompatible, and bioconjugatible $NaYF_4:Yb^{3+}/Tm^{3+}/Er^{3+}$@OCMC UC luminescence nanoparticles. Targeted cell UC luminescence imaging tests demonstrate that these UCNPs are highly desirable for biomedical applications. This facile strategy may open up a new way to the synthesis of other functional nanomaterials coated with a biocompatible shell and find great potentials in biomedical fields.

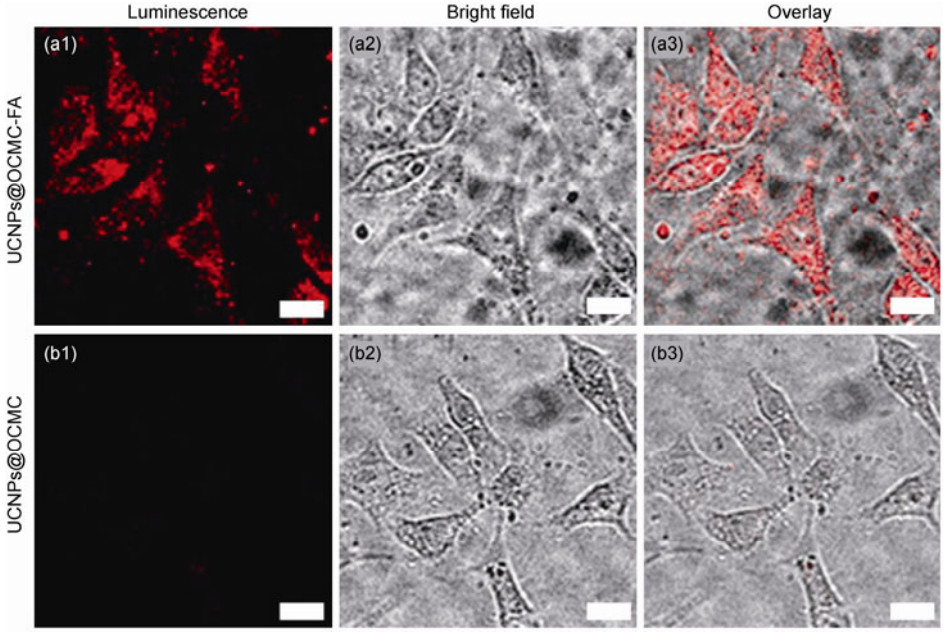

Figure 7 Confocal UC luminescence imaging of HeLa cells incubated with 75 μg/mL of $NaYF_4:Yb^{3+}/Tm^{3+}/Er^{3+}$@OCMC-FA ((a1),(a2),(a3)) and $NaYF_4:Yb^{3+}/Tm^{3+}/Er^{3+}$@OCMC ((b1),(b2),(b3)) nanoparticles, respectively. (a1),(b1) are images in dark field; (a2),(b2) are luminescence images in bright field; and (a3),(b3) are overlays of the (a1) and (a2), (b1) and (b2), respectively. All the scale bars are 20 μm. Irradiation: 980 nm.

This work was supported in part by the National Natural Science Foundation of China (21275015, 21075009), the National Basic Research Program of China (2011CB932403), and the Program for New Century Excellent Talents in University of China (NCET-10-0213).

1 Zhao Z X, Han Y N, Lin C H, et al. Multifunctional core-shell upconverting nanoparticles for imaging and photodynamic therapy of liver cancer cells. Chem-Asian J, 2012, 7: 830–837
2 Zhang F, Braun G B, Pallaoro A, et al. Mesoporous multifunctional upconversion luminescent and magnetic "nanorattle" materials for targeted chemotherapy. Nano Lett, 2012, 12: 61–67
3 Deng M L, Ma Y X, Huang S, et al. Monodisperse upconversion $NaYF_4$ nanocrystals: Syntheses and bioapplications. Nano Res, 2011, 4: 685–694
4 Zhu X J, Zhou J, Chen M, et al. Core-shell Fe_3O_4@$NaLuF_4$:Yb,Er/Tm nanostructure for MRI, CT and upconversion luminescence tri-modality imaging. Biomaterials, 2012, 33: 4618–4627
5 Xing H Y, Bu W B, Zhang S J, et al. Multifunctional nanoprobes for upconversion fluorescence, MR and CT trimodal imaging. Biomaterials, 2012, 33: 1079–1089
6 Wei Y C, Chen Q, Wu B Y, et al. High-sensitivity *in vivo* imaging for tumors using a spectral up-conversion nanoparticle $NaYF_4$:Yb^{3+}, Er^{3+} in cooperation with a microtubulin inhibitor. Nanoscale, 2012, 4: 3901–3909
7 Wang Z L, Hao J H, Chan H L W, et al. A strategy for simultaneously realizing the cubic-to-hexagonal phase transition and controlling the small size of $NaYF_4$:Yb^{3+},Er^{3+} nanocrystals for *in vitro* cell imaging. Small, 2012, 8: 1863–1868
8 Liu Q, Yang T S, Feng W, et al. Blue-emissive upconversion nanoparticles for low-power-excited bioimaging *in vivo*. J Am Chem Soc, 2012, 134: 5390–5397
9 Kuningas K, Rantanen T, Ukonaho T, et al. Homogeneous assay technology based on upconverting phosphors. Anal Chem, 2005, 77: 7348–7355
10 Gong W, Su R X, Li L, et al. A near-infrared fluorescent probe for fluorine ions and its application in the imaging of HepG2 cells. Chin Sci Bull, 2011, 56: 3260–3265
11 Zhao J Z, Ji S M, Guo H M. Triplet-triplet annihilation based upconversion: From triplet sensitizers and triplet acceptors to upconversion quantum yields. RSC Adv, 2011, 1: 937–950
12 Liu E Z, Fan J, Hu X Y, et al. Upconversion properties of sodium and aluminum fluorides coated BaF_2 material. Spectrosc Spectr Anal, 2012, 32: 61–64
13 Kramer K W, Biner D, Frei G, et al. Hexagonal sodium yttrium fluoride based green and blue emitting upconversion phosphors. Chem Mat, 2004, 16: 1244–1251
14 Wang L Y, Li Y D. Controlled synthesis and luminescence of lanthanide doped $NaYF_4$ nanocrystals. Chem Mat, 2007, 19: 727–734
15 Peng J J, Sun Y, Liu Q, et al. Upconversion nanoparticles dramatically promote plant growth without toxicity. Nano Res, 2012, 5: 770–782
16 Ang L Y, Lim M E, Ong L C, et al. Applications of upconversion nanoparticles in imaging, detection and therapy. Nanomedicine, 2011, 6: 1273–1288
17 Zhou J, Sun Y, Du X X, et al. Dual-modality *in vivo* imaging using rare-earth nanocrystals with near-infrared to near-infrared (NIR-to-NIR) upconversion luminescence and magnetic resonance properties. Biomaterials, 2010, 31: 3287–3295
18 Heer S, Wermuth M, Kramer K, et al. Sharp E-2 upconversion luminescence of Cr^{3+} in $Y_3Ga_5O_{12}$ codoped with Cr^{3+} and Yb^{3+}. Phys Rev B, 2002, 65: 5112
19 Duan Z C, Zhang J J, Xiang W D, et al. Multicolor upconversion of Er^{3+}/Tm^{3+}/Yb^{3+} doped oxyfluoride glass ceramics. Mater Lett, 2007, 61: 2200–2203
20 Wang G F, Peng Q, Li Y D. Luminescence tuning of upconversion nanocrystals. Chem-Eur J, 2010, 16: 4923–4931
21 Wang L Y, Li Y D. $Na(Y_{1.5}Na_{0.5})F$-6 single-crystal nanorods as multicolor luminescent materials. Nano Lett, 2006, 6: 1645–1649
22 Wang L Y, Zhang Y, Zhu Y Y. One-pot synthesis and strong near-infrared upconversion luminescence of poly(acrylic acid)-functionalized YF_3:Yb^{3+}/Er^{3+} nanocrystals. Nano Res, 2010, 3: 317– 325
23 Wang L Y, Li Y D. Green upconversion nanocrystals for DNA detection. Chem Commun, 2006, 2557–2559
24 Deng M L, Tu N, Bai F, et al. Surface functionalization of hydrophobic nanocrystals with one particle per micelle for bioapplications. Chem Mat, 2012, 24: 2592–2597
25 Dai Y L, Ma P A, Cheng Z Y, et al. Up-conversion cell imaging and pH-induced thermally controlled drug release from $NaYF_4$:Yb^{3+}/Er^{3+}@hydrogel core-shell hybrid microspheres. ACS Nano, 2012, 6: 3327–3338
26 Wang M, Mi C C, Wang W X, et al. Immunolabeling and NIR-excited fluorescent imaging of HeLa cells by using $NaYF_4$:Yb,Er upconversion nanoparticles. ACS Nano, 2009, 3: 1580–1586
27 Hou Z Y, Li C X, Ma P A, et al. Up-conversion luminescent and porous $NaYF_4$:Yb^{3+}, Er^{3+}@SiO_2 nanocomposite fibers for anti-cancer drug delivery and cell imaging. Adv Funct Mater, 2012, 22: 2713–2722
28 Li Z Q, Zhang Y, Jiang S. Multicolor core/shell-structured upconversion fluorescent nanoparticles. Adv Mater, 2008, 20: 4765–4769
29 Jin J F, Gu Y J, Man C W Y, et al. Polymer-coated $NaYF_4$:Yb^{3+}, Er^{3+} upconversion nanoparticles for charge-dependent cellular imaging. ACS Nano, 2011, 5: 7838–7847
30 Li J, He Y J, He Z, et al. Synthesis of $NaYF_4$:Yb,Er/single-walled carbon nanohorns nanocomposite and its application as cells label. Anal Biochem, 2012, 428: 4–6
31 Chen Z G, Chen H L, Hu H, et al. Versatile synthesis strategy for carboxylic acid-functionalized upconverting nanophosphors as biological labels. J Am Chem Soc, 2008, 130: 3023–3029
32 Naccache R, Vetrone F, Mahalingam V, et al. Controlled synthesis and water dispersibility of hexagonal phase $NaGdF_4$:Ho^{3+}/Yb^{3+} nanoparticles. Chem Mat, 2009, 21: 717–723
33 Anitha A, Rani V V D, Krishna R, et al. Synthesis, characterization, cytotoxicity and antibacterial studies of chitosan, *O*-carboxymethyl and *N*,*O*-carboxymethyl chitosan nanoparticles. Carbohydr Polym, 2009, 78: 672–677
34 An M Y, Cui J B, He Q, et al. Down-/Up-conversion luminescence nanocomposites for dual-modal cell imaging. J Mat Chem B, 2013, 1: 1333–1339
35 Pellegrino T, Manna L, Kudera S, et al. Hydrophobic nanocrystals coated with an amphiphilic polymer shell: A general route to water soluble nanocrystals. Nano Lett, 2004, 4: 703–707
36 Wang L Y, Yan R X, Hao Z Y, et al. Fluorescence resonant energy transfer biosensor based on upconversion-luminescent nanoparticles. Angew Chem Int Edit, 2005, 44: 6054–6057
37 Zhou A G, Wei Y C, Wu B Y, et al. Pyropheophorbide A and c(RGDyK) comodified chitosan-wrapped upconversion nanoparticle for targeted near-infrared photodynamic therapy. Mol Pharm, 2012, 9: 1580–1589